

IEICE **TRANSACTIONS**

on Communications

VOL. E103-B NO. 10
OCTOBER 2020

The usage of this PDF file must comply with the IEICE Provisions on Copyright.

The author(s) can distribute this PDF file for research and educational (nonprofit) purposes only.

Distribution by anyone other than the author(s) is prohibited.

A PUBLICATION OF THE COMMUNICATIONS SOCIETY



The Institute of Electronics, Information and Communication Engineers
Kikai-Shinko-Kaikan Bldg., 5-8, Shibakoen 3chome, Minato-ku, TOKYO, 105-0011 JAPAN

PAPER

DOA-Based Weighted Spatial Filter Design for Sum and Difference Composite Co-Array*

Sho IWAZAKI[†], Shogo NAKAMURA[†], *Student Members*, and Koichi ICHIGE^{†a)}, *Member*

SUMMARY This paper presents a weighted spatial filter (WSF) design method based on direction of arrival (DOA) estimates for a novel array configuration called a sum and difference composite co-array. A sum and difference composite co-array is basically a combination of sum and difference co-arrays. Our configuration can realize higher degrees of freedom (DOF) with the sum co-array part at a calculation cost lower than those of the other sparse arrays. To further enhance the robustness of our proposed sum and difference composite co-array we design an optimal beam pattern by WSF based on the information of estimated DOAs. Performance of the proposed system and the DOA estimation accuracy of close-impinging waves are evaluated through computer simulations.

key words: array antenna, adaptive beamforming, direction of arrival estimation

1. Introduction

Adaptive beamforming by an array antenna plays an important role in radar, sonar, and indoor/outdoor wireless communications [1]–[3]. Direction-of-arrival (DOA) estimation is also effective in accurately detecting the directions of array input signals, and several accurate algorithms for doing so have been proposed [4]–[6]. These methods are based on the eigenvalue decomposition of the sample covariance matrix of the array input signal, which can be regarded as algorithms with the degree of freedom (DOF) of $O(N)$, where N denotes the number of antenna elements.

There have been many studies on minimum redundancy arrays (MRAs) and methods using fourth-order cumulants to enhance the DOF [7]. However, MRAs often require very complicated computation for optimizing the array configuration. Also, the fourth-order cumulant approach can be utilized only if the signals are non-Gaussian. The concept of the Khatri-Rao (KR) product [8]–[11] assumes a quasi-stationary process and gives a difference co-array (which forms part of a larger virtual array aperture) with the DOF of $(2N - 1)$, but it cannot be used with the stationary process. Nested and co-prime arrays [12]–[15] have attracted attention as difference co-arrays, and the two-level nested array can achieve the DOF of $O(N^2)$. However, the maximum DOF of these configurations is limited to $N(N - 1) + 1$.

We previously proposed a novel array configuration

Manuscript received October 15, 2019.

Manuscript revised February 26, 2020.

Manuscript publicized April 21, 2020.

[†]The authors are with Department of Electrical and Computer Engineering, Yokohama National University, Yokohama-shi, 240-8501 Japan.

*Preliminary version of this paper is presented in [20], [21].

a) E-mail: koichi@ynu.ac.jp

DOI: 10.1587/transcom.2019EBP3213

called a “sum and difference composite co-array” that combines the sum and difference co-arrays and evaluated its beamforming performance [16]–[21]. Compared with other array configurations [22]–[24], our configuration enables a longer continuous part in a virtual array, which means higher DOF and lower calculation cost on the sum co-array part. Additionally, we introduced an array system to manage digital modulation/demodulation for the extended array and its transmission/reception procedure and evaluated the whole digital communication performance by means of bit error ratio (BER) even though most conventional systems only make and evaluate the spectrum/beam pattern on the DOA estimation/beamforming. Furthermore, we have also evaluated these benefits by estimating DOAs [20], [21].

In this paper, we further enhance robustness of our proposed system about sum and difference composite co-array by integrating the above verified DOA estimation into the beamformer, assuming that optimal beam patterns can be designed with optimal weighted spatial filter (WSF) design instead of our previous study as an example by Diagonal Loading (DL) and minimum variance distortionless response (MVDR) beamforming to realize its main-beam and null steering that can greatly suppress interference waves. In addition, as a benefit of the DOF increase from the viewpoint of higher spatial resolution, the proposed composite co-array’s capability for closed wave detection is also evaluated in this paper. This capability is linked to the next stage of WSF design with sharp and precise null characteristics.

The rest of the paper is organized as follows. In Sect. 2, we briefly introduce the signal models of a general difference co-array and our previously proposed sum and difference co-array. Section 3 describes the concept of the proposed array system based on the DOA plus WSF. After presenting the simulation results in Sect. 4, we conclude with a brief summary and mention future work in Sect. 5.

2. Preliminaries

In this section, we first prepare the basic signal model of the difference co-array. Then we briefly review the sum and difference composite co-array.

2.1 Signal Model of Difference Co-Array

Consider an N -element uniform linear array (ULA) with the signal model given by $N \times 1$ array steering vector $\mathbf{a}(\theta)$ corresponding to the phase delays of each array input $e^{j(2\pi/\lambda)d_p \sin \theta}$

that comes from the direction of θ_i at the p -th element. Here, the parameter λ is the wavelength of the carrier wave and $d_p = p \cdot d$ is the distance between the reference (first) and the p -th element positions where $d = \lambda/2$.

We assume D narrowband input waves impinging on this array with the powers $\{\sigma_i^2, i = 1, 2, \dots, D\}$ from the directions $\{\theta_i, i = 1, 2, \dots, D\}$, respectively; then, the received signal vector $\mathbf{x}(k) = [x_1(k), x_2(k), \dots, x_N(k)]^T$ is written as

$$\mathbf{x}(k) = \mathbf{A}\mathbf{s}(k) + \mathbf{n}(k), \quad (1)$$

where the matrix $\mathbf{A} = [\mathbf{a}(\theta_1), \mathbf{a}(\theta_2), \dots, \mathbf{a}(\theta_D)]$ expresses the array manifold matrix and $\mathbf{s}(k) = [s_1(k), s_2(k), \dots, s_D(k)]^T$ is the plane source signal vector whose signals $s_i(k)$ are uncorrelated and is temporally uncorrelated with itself. Its elements generally take complex values. The vector $\mathbf{n}(k) = [n_1(k), n_2(k), \dots, n_N(k)]^T$ is a noise vector that has temporally and spatially white Gaussian signals that are uncorrelated in this case. The autocorrelation matrix of the array input vector $\mathbf{x}(k)$ is denoted as

$$\begin{aligned} \mathbf{R}_{xx} &= E[\mathbf{x}(k)\mathbf{x}^H(k)] = \mathbf{A}\mathbf{R}_{ss}\mathbf{A}^H + \sigma^2\mathbf{I}_N \\ &\simeq \mathbf{A} \begin{bmatrix} \sigma_1^2 & & & O \\ & \sigma_2^2 & & \\ & & \ddots & \\ O & & & \sigma_D^2 \end{bmatrix} \mathbf{A}^H + \sigma^2\mathbf{I}_N, \end{aligned} \quad (2)$$

where $\mathbf{R}_{ss} = E[\mathbf{s}(k)\mathbf{s}^H(k)] \in \mathbb{R}^{D \times D}$, $\mathbf{A} \in \mathbb{C}^{N \times D}$, σ^2 denotes the noise power and $\mathbf{I}_N \in \mathbb{R}^{N \times N}$ denotes the identity matrix. Then, we vectorize the matrix \mathbf{R}_{xx} as

$$\begin{aligned} \mathbf{z} &= \text{vec}(\mathbf{R}_{xx}) = (\mathbf{A}^* \odot \mathbf{A})\mathbf{p} + \sigma^2\mathbf{1}_N \\ &= \text{vec} \left\{ \sum_{i=1}^D \sigma_i^2 (\mathbf{a}(\theta_i)\mathbf{a}^H(\theta_i)) \right\} + \sigma^2\mathbf{1}_N, \end{aligned} \quad (3)$$

where $\mathbf{1}_N = [\mathbf{e}_1^T, \mathbf{e}_2^T, \dots, \mathbf{e}_N^T]^T \in \mathbb{R}^{N^2 \times 1}$, $\mathbf{p} = [\sigma_1^2, \sigma_2^2, \dots, \sigma_D^2]^T \in \mathbb{R}^{D \times 1}$, and \odot denote the Khatri-Rao product operator. In the unit vector $\mathbf{e}_i \in \mathbb{R}^{N \times 1}$, the i -th column is one, and all the others are zero. The column component of $\mathbf{A}^* \odot \mathbf{A} \in \mathbb{C}^{N^2 \times D}$ needs to enable us to represent the extended array steering vector, which includes the set of virtual sensor positions $\{d_p - d_q \mid 1 \leq p, q \leq N\}$. This form is called the difference co-array and can be applied to DOA estimation, adaptive beamforming, and so on. Also, the difference co-array behaves in accordance with the second-order statistics of the input vector, such that σ_i^2, σ_j^2 ($i \neq j$) behave like coherent signals to each other. An earlier study [12] showed that the maximum DOF in that case is given by $\text{DOF}_{\text{Diff-Max}} = N(N-1) + 1$.

Furthermore, we remove redundant rows from the above manifold $\mathbf{A}^* \odot \mathbf{A}$ and replace the rows that correspond to the locations of virtual elements in ascending order. Let us denote this matrix as $\mathbf{A}_1 \in \mathbb{C}^{N_1 \times D}$, where $N_1 = N^2/2 + N - 1$ in the case of even N . Then, the new observation vector $\mathbf{z}_1 \in \mathbb{C}^{N_1 \times 1}$ whose elements are in order without redundancy is given by $\mathbf{z}_1 = \mathbf{A}_1\mathbf{p} + \sigma^2\hat{\mathbf{e}}$,



Fig. 1 Construction of six-element nested array.

where $\hat{\mathbf{e}} \in \mathbb{R}^{N_1 \times 1}$ is a vector of all zeros except one at the $(N^2/4 + N/2)$ -th position. The configuration of the nested array [12], which is common example of a difference co-array, is shown in Fig. 1.

2.2 Sum and Difference Composite Co-Array [19]–[21]

Now we introduce our previously proposed novel array configuration [20], the sum and difference composite co-array, and show its numerical model.

The key fact here is that the manifold $(\mathbf{a}^*(\theta_i) \otimes \mathbf{a}(\theta_i))$ represents the array steering vector of the virtual elements that compose the difference co-array. Assume that the desired wave takes real values that satisfy $s_s(k) = s_s^*(k)$, as in [19]. That is, the relation $\bar{\sigma}_1^2 = \sigma_1^2$ holds and we can realize the sum co-array for the desired signal. In this case, the matrix $\bar{\mathbf{R}}_{xx}$ is written as

$$\bar{\mathbf{R}}_{xx} = E[\mathbf{x}(k)\mathbf{x}^T(k)] = \mathbf{A}\bar{\mathbf{R}}_{ss}\mathbf{A}^T + \bar{\sigma}^2\mathbf{I}_N, \quad (4)$$

where $\bar{\mathbf{R}}_{ss}$ is the correlation matrix corresponding to the real-valued signal \bar{s} . Then, the observation vector $\bar{\mathbf{z}} = \text{vec}(\bar{\mathbf{R}}_{xx})$ includes the extended array steering vector of the sum co-array. Here, the proposed array configuration is expressed as Fig. 2 and also formulated as below:

$$d_p = pd, \quad (0 \leq p \leq N/2 - 1), \quad (1\text{st-level}), \quad (5)$$

$$\begin{aligned} d_{\alpha_p} &= \{N/2 + p(N-1)\}d \\ &= \alpha_p d, \quad (1 \leq p \leq N/2), \quad (2\text{nd-level}). \end{aligned} \quad (6)$$

For positive positions, 0 and negative directions can be created that are more than or equal to $N_2 = (N+1)N + 1$ virtual components that appear continuously, which has the significant advantage of enhancing DOF compared with other extended arrays. The extended input vector $\bar{\mathbf{z}} = [\mathbf{z}^T, \bar{\mathbf{z}}^T, \check{\mathbf{z}}^T]^T \in \mathbb{C}^{3N^2 \times 1}$ corresponds to the power of the extended difference co-arrays, the sum co-arrays for the positive direction, and the sum co-arrays for the negative direction.

For an application, we have studied minimum variance distortionless response (MVDR) beamforming with diagonal loading (DL) [16], [19]. Considering the beamforming via the weight vector $\bar{\mathbf{w}}_{\text{MVDR}} \in \mathbb{C}^{N_2 \times 1}$, its signal model of array output is described as $y_{\text{MVDR}} = \bar{\mathbf{w}}_{\text{MVDR}}^H \bar{\mathbf{z}}$, where $\bar{\mathbf{w}}_{\text{MVDR}}$ is composed of the weight vector of the sum and difference composite co-array corresponding to that of $\bar{\mathbf{z}}$, and is derived by the solution of an optimization problem on the MVDR beamformer. This will lead to more robust performance in the case of less snapshot and also has the great advantage that we can keep the DOF without any spatial smoothing method.

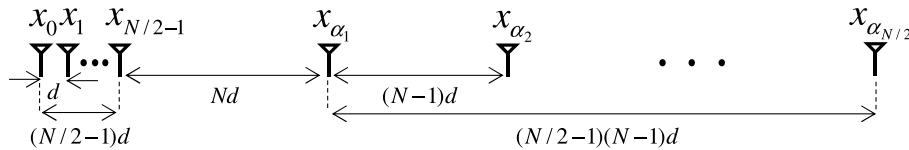


Fig. 2 Construction of N -element sum and difference co-array.

3. Proposed Array System

In order to enhance the beamforming performance of the array configuration in Sect. 2.2, we employ DOA estimation to suppress close-angle interference waves. We adopt “DOA estimation + WSF” approach to improve robustness of beamforming performance to suppress interference waves, as well as enhancing whole modulation/demodulation system performance. Note that we do not aim at reducing the computational cost but developing a system which improves beamforming and modulation performance.

3.1 Application to DOA Estimation Method

The extended input vector \bar{z} in 2.2 corresponds to the power of the physical array inputs, and we also consider the DOA estimation via the spatially smoothed autocorrelation matrices $\bar{\mathbf{R}}_{SS}$ of \bar{z} , which is expressed as \mathbf{R}_{SS} in our previous work [19]. \bar{z} may have another snapshot or vector size different from \bar{z} from the viewpoint of calculation cost, real-time response, or accuracy that we can use, and in the following sentence accent $\bar{[\cdot]}$ also includes capability for another snapshot relative to $[\cdot]$ where $[\cdot]$ describes arbitrary character. \bar{z} is for recovering the signal and deducing the $\bar{\mathbf{R}}_{DL}$ for MVDR Beamforming in 2.2. Now we consider applying $\bar{\mathbf{R}}_{SS}$ to the spatially smoothing multiple signal classification (SS-MUSIC) method as an example of the subspace-based DOA estimation method. As a result, we can obtain the estimated DOAs of the impinging signals $\bar{\theta} : \{\bar{\theta}_i, i = 1, 2, \dots, D\}$, which is very useful information that we will use in the next subsection.

3.2 Application to Weighted Spatial Filter Design

Now we can treat the DOAs of impinging waves $\bar{\theta} : \bar{\theta}_i, i = 1, 2, \dots, D$, which include useful information of the desired wave and the interference waves, via the SS-MUSIC method [12] with higher spatial resolution through the virtual array enhancement coming from the proposed system [20]. Hence, we consider a more effective spatial filter design to extract the desired wave on the basis of the null design to suppress interference waves more strongly. Then the filter design according to the weighted cost function and based on the least squares principle can be expressed through the following formulae:

$$C = C_1 + C_2$$

$$= \sum_{\omega = -\omega_s}^{\omega_s} \left\| H(\omega) - \sum_{n=-N_V}^{N_V} h(n)e^{-j\omega n} \right\|^2 + \sum_{\omega \in \Omega} v_i \left\| H(\omega) - \sum_{n=-N_V}^{N_V} h(n)e^{-j\omega n} \right\|^2, \quad (7)$$

where C_1 part is the standard and non-weighted cost function of filter design based on the least square norm, $H(\omega)$ is the amplitude of the ideal filter, especially $\omega_s = 2\pi d \sin \theta / \lambda = \pi \sin \theta$, $\theta \in [-\pi/2, \pi/2]$ is the spatial angular frequency, and N_V is the array number of the continuous part in the virtual array. $h(n)$ is generally regarded as impulse response of the filter or system we are planning to design and also corresponds to adaptive weights of an extended array such as $w_{\text{Diff},n}$ or \bar{w}_n . Additionally, in the description of the efficiency of the cost function part C_2 , v_i means its weight, which represents the significance of the amplitude/power on DOAs $\bar{\theta}_i$ of all impinging waves (desired wave and interference waves) in these spatial angular frequency domains $\Omega \in \{\omega_{s,i}, i = 1, 2, \dots, D\}$ compared with the significance of the amplitude/power in other directions. The reason the least squares norm is selected this time is, especially considering the C_1 part, the term effect to outline the filter shape. We can also choose other norms, for example the ℓ_∞ -norm, which is common in minimax filter design. However, the goal of the spatial filter design this time is to realize a filter design not with smooth areas but with a flexible and sharp pattern to acquire or reject each impinging wave effectively. It may be more applicable to use another form for C_2 . Discussing beampatterns, the optimal design problem of filter coefficients $h(n)$ can be regarded as the optimal beampattern design problem. Provided that the beamformer is not realized by the frequency with uniform interval of $e^{-j\omega n}$ like Discrete Fourier Transform (DFT) but described as the summation multiplied by $e^{j(2\pi/\lambda)d_p \sin \theta}$ with every direction of θ . That is, design of the ideal filter $H(\omega)$ on the frequency domain must ensure that the desired beam-response is acquired after transformation by spatial frequency $d \sin \theta / \lambda = \sin \theta / 2$.

This time, we will introduce the actual filter design procedure as follows (i) - (iii). The weighted cost function concept of (7) is used to create the prototype low pass filter (LPF) $h(n)$, and a frequency shift method is used as an example of the optimal filter design that can generate \bar{w}_{WSF} .

- (i) In the prototype LPF design, pass band corresponds to around 0° in the DOA domain initially.

$$\gamma_i = \left| \bar{\theta}_i - \bar{\theta}_1 \right|, \quad (8)$$

should be new target angles of the prototype LPF. Note

that we should also design the null patterns in accordance with the DOAs of interference waves on the prototype LPF in preparation for next process of frequency shift.

- (ii) The normalized target frequency of the ideal filter corresponding to angles or spatial frequency shall be given the function on $\sin\gamma$. Therefore, normalized frequency for the standard filter design will be linear treating not time or space samples but spatial frequency on the array antenna defined by $\sin\{\cdot\}$ stated as above. The cost function of the optimal design problem is:

$$C_\gamma = C_{\gamma,1} + C_{\gamma,2}$$

$$= \sum_{\gamma=0}^{\pi/2} \left\| H(\sin\gamma) - \sum_{n=-N_V}^{N_V} h(n)e^{-jns\sin\gamma} \right\|^2$$

$$+ \sum_{\gamma \in \Gamma} v_i \left\| H(\sin\gamma) - \sum_{n=-N_V}^{N_V} h(n)e^{-jns\sin\gamma} \right\|^2, \quad (9)$$

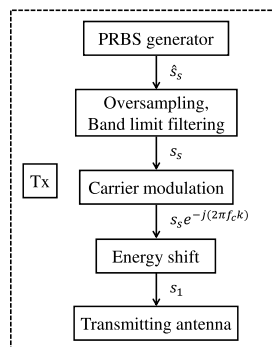
where $\Gamma \in \{\gamma_i, i = 1, 2, \dots, D\}$, here $C_{\gamma,1}$ and $C_{\gamma,2}$ parts of C_γ have similar roles to C_1 and C_2 of C in (7).

- (iii) After the prototype LPF is formed, pass band (=main beam) can be shifted on the basis of the DOA of the desired wave $\bar{\theta}_1$ to adjust pass band by applying the frequency shift approach in concert with other parts including nulls, which is achieved with multiplied by $e^{-j(2\pi/\lambda)d_p \sin \bar{\theta}_1}$ to every point of p . Because we defined the array output as $y_{\text{WSF}} = \bar{\mathbf{w}}_{\text{WSF}}^H \bar{\mathbf{z}}$, weight vectors are considered to be a conjugated operation on filtering. Thus, we should apply phase shift to the flip-side prior to output filtering.

As a result, we can design the $\bar{\mathbf{w}}_{\text{WSF}}$ with the desired accurate and precise specifications for robust beamforming.

3.3 System Configuration

Figure 3(a) shows a transmitter (Tx) system model of our previously proposed beamformer [19]. We first generate the symbol sequence $\hat{s}_s(k)$ as a pseudo random signal of binary phase shift keying (BPSK), and then the sequence $\hat{s}_s(k)$ is

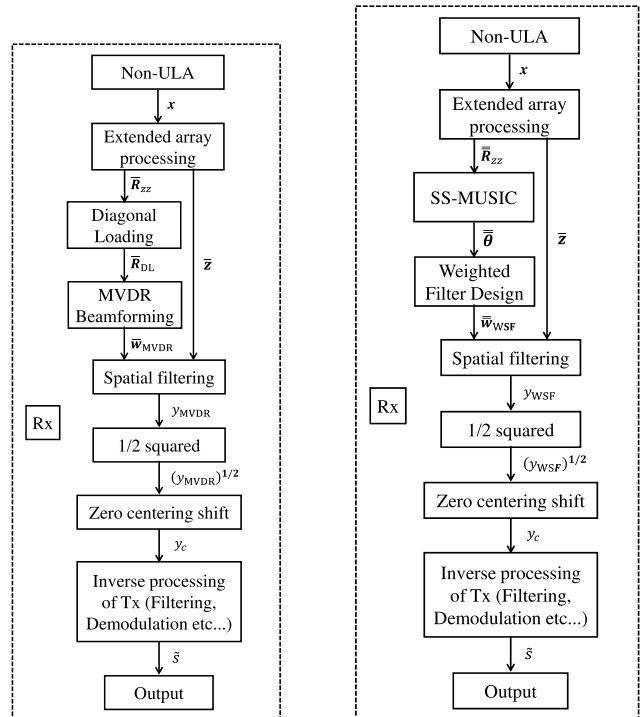


(a) Tx system model

Fig. 3 Tx system model of simulations.

filtered into $s_s(k)$ by using a root-cosine rolloff filter after oversampling to avoid any problems caused by inter symbol interference (ISI). After that, the carrier wave $e^{-j(2\pi f_c k)}$ is multiplied to $s_s(k)$ and then transmitted from the transmission antenna. Note that the center value of the amplitude is shifted to 1 to avoid negative amplitudes for squared extended array operation, i.e., $s_1(k) = s_s(k)e^{-j(2\pi f_c k)} + 1$. This amplitude allocated in a positive quadrant works effectively; indeed, we do not have to distinguish whether squared signals were originally positive or not.

In the receiver (Rx) system in Fig. 4(a), also discussed previously [19], the weight $\bar{\mathbf{w}}_{\text{MVDR}}$ and the extended signal $\bar{\mathbf{z}}$ are used to recover the output signal $\bar{s} \approx \hat{s}_s$. In contrast, Fig. 4(b) shows the new system proposed in this paper based on the procedure of SS-MUSIC and WSF design in Sect. 3.2 $\bar{\mathbf{w}}_{\text{WSF}}$ can be adopted instead of $\bar{\mathbf{w}}_{\text{MVDR}}$. Provided that the number of snapshots used in the autocorrelation process (2) and (3) are within a symbol period, their snapshots are often common (but could be different) for the generating processes of $\bar{\mathbf{w}}_{\text{MVDR}}$ in Sect. 2.2, $\bar{\mathbf{w}}_{\text{WSF}}$ based on (7) and $\bar{\mathbf{z}}$ in (3). As a reminder, we will replace the variables $\bar{\mathbf{R}}_{zz}$, $\bar{\boldsymbol{\theta}}$ and $\bar{\mathbf{w}}_{\text{WSF}}$ with $\bar{\mathbf{R}}_{zz}$, $\bar{\boldsymbol{\theta}}$ and $\bar{\mathbf{w}}_{\text{WSF}}$ so that capabilities for different snapshots makes more sense. Then, we transform the spatial filtered output y_{MVDR} and y_{WSF} containing powered behaviors into the original amplitude expression by means of the square-root operation. The output y_c is acquired by the zero-centering shift operation, and now we use the temporal average of $(y_{\text{MVDR}})^{1/2}$ or $(y_{\text{WSF}})^{1/2}$ as an example of a shift operator. After that, we apply the inverse processing of



(a) DL+MVDR

(b) SS-MUSIC+WSF

Fig. 4 Rx system models of simulations.

Tx, which includes the carrier wave rejection by multiplying the phase-term $e^{j(2\pi f_s k)}$, the root-cosine rolloff filtering, and the decimation. As a result, the processed output signal $\tilde{s}(k)$ is obtained. In the next section, it is compared with the ideal source symbol sequence $\hat{s}_s(k)$ in terms of BER performance.

4. Simulation

The performances of the proposed array configuration and new array system are evaluated through computer simulation in this section. We have already studied the DOA estimation performance in case of $N \leq D$ in [20], i.e., case of more number of sources D than the number of physical elements N . In this paper, we rather focus on the effect of larger DOF to angular resolution, i.e., beamforming performance in case of multiple close-angle waves. Also note that we use MUSIC method as a DOA estimator but the WSF also works if it is used with any other accurate DOA estimation method.

4.1 Evaluation of the DOA Performance Toward the Close Impinging Wave

Robustness and accuracy on the proposed array in the DOA estimation for the close wave are evaluated and compared with those of the nested array. Specifications of the simulation are listed in Table 1.

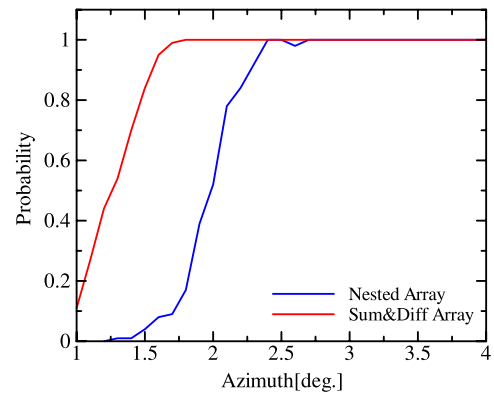
First, characteristics for spatial resolution that express the capability for closed wave detection are evaluated. Here, we try to sweep one of the DOAs of the interference wave from 1° to 4° as shown in Figs. 5(a) and 6(a). Note that probabilities are considered in accordance with the threshold we set. If all root mean square errors (RMSEs) are ≤ 1 for each estimated peak between the ideal DOAs, the estimation is defined as a success. However, if at least one RMSE exceeds 1, the estimation is defined as a failure. Moreover, results in Fig. 6(a) are calculated and plotted by the limited case probabilities of 1.

Figures 5(a) and 6(a) show that the proposed sum & diff array performs better than the conventional nested array for the whole range. In Fig. 5(a), the probability is 100% when 1.8° with the sum & diff array but 2.4° with the nested array, which is a 0.6° improvement in the spatial resolution. Figure 6(a) confirms the better accuracy of the sum & diff array. For example, RMSEs are 5.70 and 2.82 times higher at 2.4° and 4° , respectively.

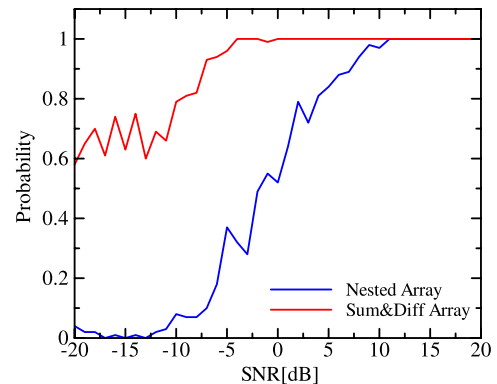
In addition, Figs. 5(b) and 6(b) denote the case when the azimuth of the interference wave is fixed at 2° . Then we can verify that in Fig. 5(b) the probability reaches 100% around -3 dB and 11 dB from the viewpoint of signal-to-noise ratio (SNR). Therefore, the proposed sum & diff array contributes to around 14 dB improvement and is more robust in a low SNR environment. Figure 6(a) also shows that RMSE is 5.46 times higher at an SNR of 11 dB in the same manner.

Table 1 Specifications of simulation no. 1.

Scenario	#1	#2
No. of array elements N	10	
Sensor allocations $\{p, q\}$		
Nested array	{0, 1, 2, 3, 4, 5, 11, 17, 23, 29}	
Sum&Diff array (Proposed)	{0, 1, 2, 3, 4, 14, 23, 32, 41, 50}	
No. of input signals D	3	
Array interval d_1	$\lambda/2$	
Modulation	BPSK	
DOA of desired wave	0°	
DOA of interference wave #1	-5° (fixed)	
DOA of interference wave #2	1° to 4° (swept)	2° (fixed)
SNR	0 B	-20 to 20 dB
SIR	0 dB	
No. of snapshots (for SS-MUSIC)	100	
No. of trials (for RMSE)	20	



(a) In Scenario #1

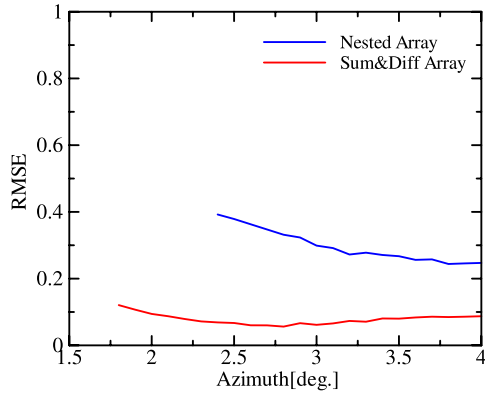


(b) In Scenario #2

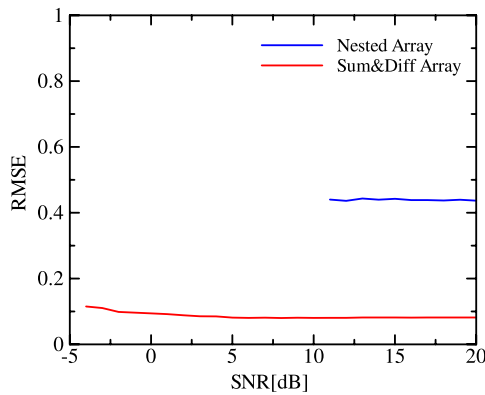
Fig. 5 Comparison of DOA estimation probability characteristics.

4.2 Evaluation of the Performance on the Array System

Here we compare the performances of the array system proposed in this paper and the previous one [19]. Specifications of the simulation are listed in Table 2, where the same 22 elements are used but allocated to different positions and have different signal processing applied to them. In case of $N = 10$ with the condition of Table 1, we can estimate DOAs

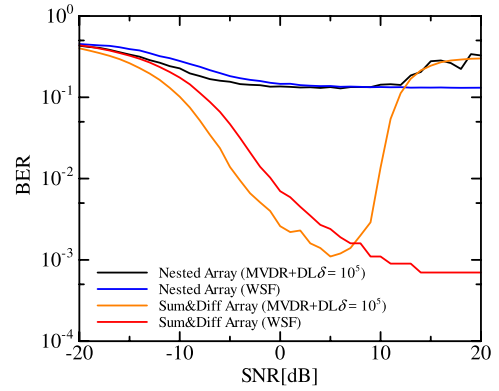


(a) In Scenario #1

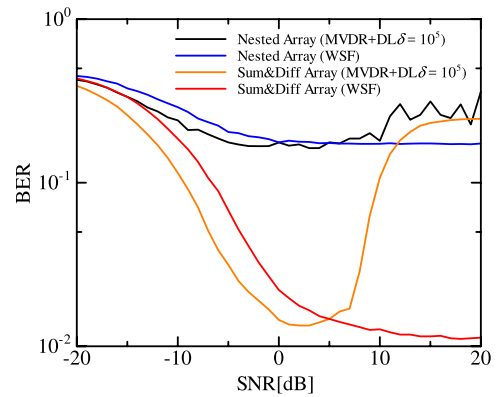


(b) In Scenario #2

Fig. 6 Comparison of DOA estimation RMSE characteristics.



(a) In Scenario #3



(b) In Scenario #4

Fig. 7 Comparison of BER characteristics for three interference waves.

Table 2 Specifications of simulation no. 2.

Scenario	#3	#4
No. of array elements N	22	
Sensor allocations $\{p, q\}$	as in [12]	
Nested array	as in (5), (6)	
Sum&Diff array (Proposed)		
No. of input signals D	3	
Array interval d_1	$\lambda/2$	
Modulation	BPSK	
DOA of desired wave	2°	
DOAs of interference waves	$-5^\circ, 0^\circ$ (fixed)	
SNR	-20 to 20 dB (Fig. 7) 0 dB (Figs. 8,9)	
SIR	3 dB	0 dB
No. of snapshots (for Beamformer)	500	
No. of snapshots (for SS-MUSIC)	3000	

as shown in Sect. 4.1 but have difficulty in beamforming due of low DOF. As far as our simulation, more than 20 physical elements are mandatory for minute beamforming in a severe condition in Table 2. Therefore we changed the value of N into a larger one $N = 22$ as in Table 2. In general, more number of physical elements are often required than the number of elements which can well estimate DOAs.

Figure 7 shows BER characteristics in case of Scenario #3 and #4. We see from Fig.7(a) that the BER charac-

teristics of the previous (MVDR+DL) method gets worse influentially in the case of $SNR \geq 5$ dB, which means slightly greater sidelobe remains because of less noise. Also the method cannot well direct null-beam to the directions of interferences. On the other hand, the proposed (SS-MUSIC+WSF) method can achieve good BER characteristics even in cases of high SNRs because of suppressing interferences via proper null steering, so better robustness is observed even in the high SNR region in which DL+MVDR cannot work well. Similar observation can be found in Fig. 7(b).

Figures 8 and 9 show the beampattern of the previous method and that of the proposed method, where red/yellow arrows denote DOAs of the desired/interference waves. We see from Figs. 8 and 9 that the previous method cannot design the null pattern well toward the interference waves because the DL method trades off its capability of main beam steering against low capability of null steering. On the other hand, the proposed method makes null beams on the DOAs of target interference waves directly and precisely without missing the direction of mainlobe because of using the estimated DOA information $\hat{\theta}_i$. The proposed method can defeat major weak points of previous and general extended array approaches.

Additionally, the proposed method has slightly less

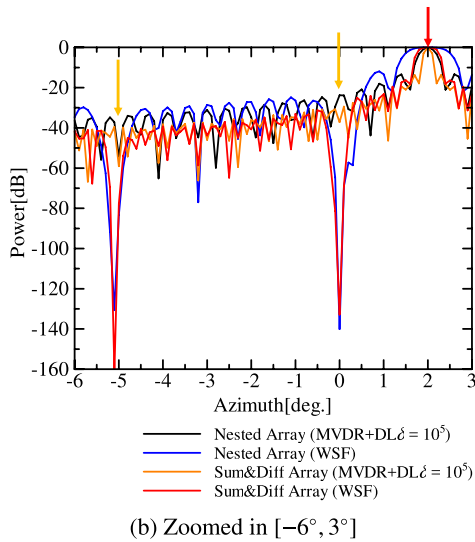
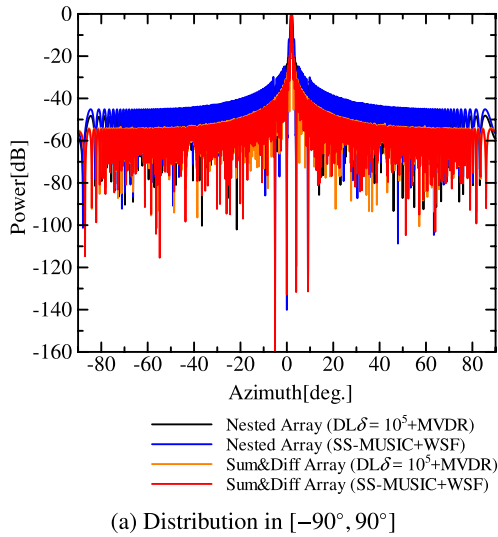


Fig. 8 Performance comparison in case of SIR 3 dB.

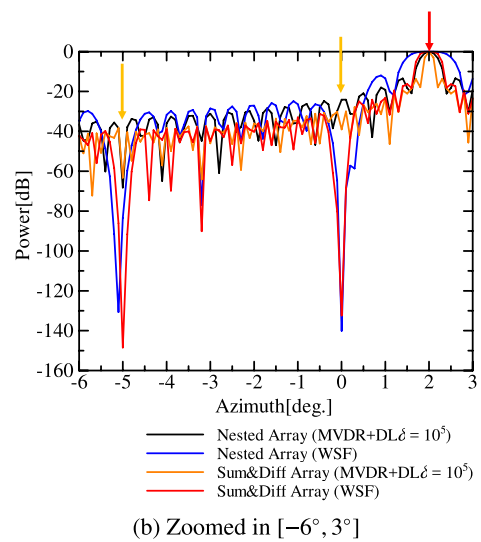
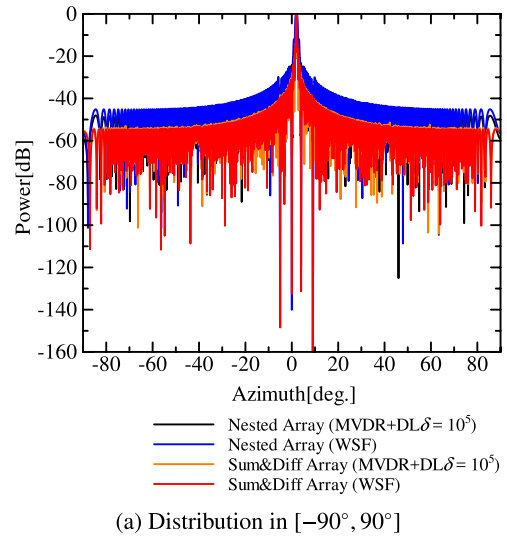


Fig. 9 Performance comparison in case of SIR 0 dB.

noise tolerance than DL+MVDR due to the slightly wider main beam, whose adverse effect may be caused by the quite strong null steering. Indeed this problem can be overcome by increasing the filter-order (corresponding to virtual element), but to evaluate the differences in performance fairly, we compared the proposed and previous systems under severe conditions.

5. Concluding Remarks

In this paper, we presented an array system that consists of spatially smoothing multiple signal classification (SS-MUSIC) and weighted spatial filter (WSF) together our previously proposed sum and difference composite co-array configuration. Because our array configuration enhances the degree of freedom (DOF), we confirmed through the computer simulation that the proposed system achieved better spatial resolution on the SS-MUSIC and more robust beamforming with WSF than our previous system due to a pre-

cise design for mainbeam/null steering toward closer interference waves.

Determining the optimal physical/virtual array number for any given purpose, and the application of the present filter approach to two-dimensional sparse arrays [25], [26] remain as our future works.

Acknowledgments

We are sincerely grateful for the support this work received from the Support Center for Advanced Telecommunications Technology Research Foundation.

References

- [1] B. Allen and M. Ghavami, Adaptive Array Systems: Fundamentals and Applications, Wiley, 2005.
- [2] C.A. Balanis and P.I. Ioannides, Introduction to Smart Antennas, Morgan & Claypool, 2007.

- [3] S. Chandran ed., *Adaptive Antenna Arrays: Trends and Applications*, Springer, 2004.
- [4] R.O. Schmidt, "Multiple emitter location and signal parameter estimation," *IEEE Trans. Antennas Propag.*, vol.34, pp.276–280, March 1986.
- [5] R.T. Hoctor and S.A. Kassam, "The unifying role of the coarray in aperture synthesis for coherent and incoherent imaging," *Proc. IEEE*, vol.78, no.4, pp.735–752, April 1990.
- [6] M.M. Hyder and K. Mahata, "Direction-of-arrival estimation using a mixed $\ell_{2,0}$ norm approximation," *IEEE Trans. Signal Process.*, vol.58, no.9, pp.4646–4655, Sept. 2010.
- [7] M.C. Dogan and J.M. Mendel, "Applications of cumulants to array processing Part I: Aperture extension and array calibration," *IEEE Trans. Signal Process.*, vol.43, no.5, pp.1200–1216, May 1995.
- [8] W.K. Ma, T.H. Hsieh, and C.Y. Chi, "DOA estimation of quasi-stationary signals via Khatri-Rao subspace," *IEEE Proc. Int. Conf. Acoustic. Speech Signal Process.*, pp.2165–2168, April 2009.
- [9] T. Terada, T. Nishimura, Y. Ogawa, T. Ohgane, and H. Yamada, "DOA estimation for multi-band signal sources using compressed sensing techniques with Khatri-Rao processing," *IEICE Trans. Commun.*, vol.E97-B, no.10, pp.2110–2117, Oct. 2014.
- [10] J. Konishi, H. Yamada, and Y. Yamaguchi, "Optimum element arrangements in MIMO radar using Khatri-Rao product virtual array processing," *IEICE Communications Express*, vol.7, no.11, pp.407–414, Nov. 2018.
- [11] K. Hayashi, M. Nagahara, and T. Tanaka, "A user's guide to compressed sensing for communications systems," *IEICE Trans. Commun.*, vol.E96-B, no.3, pp.685–712, March 2013.
- [12] P. Pal and P.P. Vaidyanathan, "Nested arrays: A novel approach to array processing with enhanced degrees of freedom," *IEEE Trans. Signal Process.*, vol.58, no.8, pp.4167–4181, Aug. 2010.
- [13] P. Pal and P.P. Vaidyanathan, "Nested arrays in two dimensions, Part I: geometrical considerations," *IEEE Trans. Signal Process.*, vol.60, no.9, pp.4694–4705, Sept. 2012.
- [14] P.P. Vaidyanathan and P. Pal, "Sparse sensing with co-prime samplers and arrays," *IEEE Trans. Signal Process.*, vol.59, no.2, pp.573–586, Feb. 2011.
- [15] Z. Tan, Y.C. Eldar, and A. Nehorai, "Direction of arrival estimation using co-prime arrays: A super resolution viewpoint," *IEEE Trans. Signal Process.*, vol.62, no.21, pp.5565–5576, Nov. 2014.
- [16] S. Iwazaki and K. Ichige, "Sum and difference composite co-array: An extended array configuration toward higher degree of freedom," *Proc. International Conference on Advances in Electrical, Electronic and Systems Engineering (ICAEESE)*, pp.351–356, Nov. 2016.
- [17] S. Iwazaki and K. Ichige, "Extended beamforming by sum and difference composite co-array for radio surveillance," *Proc. IEEE International Workshop on Information Forensics and Security (WIFS)*, no.61, Dec. 2017.
- [18] S. Iwazaki and K. Ichige, "Adaptive beamforming by array antenna via using feedback section," *IEICE Trans. Fundamentals (Japanese Edition)*, vol.J100-A, no.1, pp.70–78, Jan. 2017.
- [19] S. Iwazaki and K. Ichige, "Extended beamforming by sum and difference composite co-array for real-valued signals," *IEICE Trans. Fundamentals*, vol.E102-A, no.7, pp.918–925, July 2019.
- [20] S. Iwazaki and K. Ichige, "Underdetermined direction of arrival estimation by sum and difference composite co-array," *Proc. 25th IEEE International Conference on Electronics, Circuits and Systems (ICECS)*, pp.669–672, Dec. 2018.
- [21] S. Iwazaki and K. Ichige, "DOA-based weighted spatial filter design for sum and difference composite co-array," *Proc. 26th IEEE International Conference on Electronics, Circuits and Systems (ICECS)*, Nov. 2019.
- [22] X. Wang, Z. Chen, S. Ren, and S. Cao, "DOA estimation based on the difference and sum coarray for coprime arrays," *Digit. Signal Process.*, vol.69, pp.22–31, Oct. 2017.
- [23] X. Wang, X. Wang, and X. Lin, "Co-prime array processing with sum and difference co-array," *Proc. 49th Asilomar Conf. Signals,*

Systems and Computers, pp.380–384, Nov. 2015.

- [24] J. Liu, Y. Zhang, Y. Lu, S. Ren, and S. Cao, "Augmented nested arrays with enhanced DOF and reduced mutual coupling," *IEEE Trans. Signal Process.*, vol.65, no.21, pp.5549–5563, Nov. 2017.
- [25] S. Nakamura, S. Iwazaki, and K. Ichige, "Optimum 2D sparse array and its interpolation via nuclear norm minimization," *Proc. IEEE International Symposium on Circuits and Systems (ISCAS)*, pp.1–5, May 2019.
- [26] S. Nakamura, S. Iwazaki, and K. Ichige, "Optimum 2D sparse array and hole interpolation for accurate direction of arrival estimation," submitted to *IEICE Trans. Communications*.



Sho Iwazaki received B.E., M.E. and Dr. Eng. degrees in Electrical and Computer Engineering from Yokohama National University, Japan, in 2009, 2011 and 2020. He joined Sony Corporation in 2011 and currently with Sony Interactive Entertainment Inc. His research interests include array signal processing and its applications. He received the Best Student Paper Award in Int. Conf. on Electrical, Electronic and Systems Engineering (ICAEESE) in 2016.



Shogo Nakamura received a B.E. and M.E. degrees in Electrical and Computer Engineering from Yokohama National University, Japan, in 2018 and 2020. He joined Denso Corporation in 2020. His research interests include array antenna, DOA estimation, and digital signal processing.



Koichi Ichige received B.E., M.E. and Dr. Eng. degrees in Electronics and Computer Engineering from the University of Tsukuba in 1994, 1996 and 1999, respectively. He joined the Department of Electrical and Computer Engineering, Yokohama National University as a research associate in 1999, where he is currently a professor. He has been on leave to Swiss Federal Institute of Technology Lausanne (EPFL), Switzerland as a visiting researcher in 2001–2002. His research interests include digital signal processing, approximation theory and their applications to image processing and mobile communication. He served as an associate editor of *IEEE Transactions on Industrial Electronics* in 2004–2008, that of *Journal of Circuits, Systems and Computers (JCS)* in 2012–2014, that of *IEICE Transactions on Fundamentals of Electronics, Communications and Computer Sciences (IEICE-EA)* in 2015–2018, and currently serves as an editor of *IEICE-EA*. He received "Meritorious Award on Radio" from the Association of Radio Industries and Businesses (ARIB) in 2006, and Best Letter Award from *IEICE Communication Society* in 2007. He is a member of IEEE.